Energy Conversion and Management 268 (2022) 115963

Contents lists available at ScienceDirect

Energy Conversion and Management

journal homepage: www.elsevier.com/locate/enconman

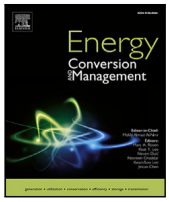

Performance assessment of an experimental CO_2 transcritical refrigeration plant working with a thermoelectric subcooler in combination with an internal heat exchanger

Álvaro Casi [a], Patricia Aranguren [a], Miguel Araiz [a,*], Daniel Sanchez [b], Ramon Cabello [b], David Astrain [a]

[a] Department of Engineering, Institute of Smart Cities, Public University of Navarre, Campus de Arrosadia s/n E-31006, Pamplona, Spain
[b] Department of Mechanical Engineering and Construction, Jaume I University, Campus de Riu Sec s/n E-12071, Castellón, Spain

ARTICLE INFO

Keywords:
Refrigeration
Transcritical
Carbon dioxide
Thermoelectric subcooler
Internal heat exchanger
COP

ABSTRACT

Regulations in the refrigeration sector are forcing the transition to low global warming potential fluids such as carbon dioxide in order to decrease direct greenhouse gases emissions. Several technologies have arisen over the past years to compensate the low performance of the transcritical carbon dioxide vapour compression cycle at high ambient temperatures. For low–medium power units, the inclusion of a thermoelectric subcooler or an internal heat exchanger have been proven as effective solutions for enhancing the coefficient of performance. However, the combination of a thermoelectric subcooler and an internal heat exchanger working simultaneously is yet to be explored theoretically or experimentally. This work presents, for the first time, an experimental transcritical carbon dioxide refrigeration facility that works simultaneously with a thermoelectric subcooler and with an internal heat exchanger in order to boost the cooling capacity and coefficient of performance of the refrigeration system. The experimental tests report improvements at optimum working conditions of 22.4 % in the coefficient of performance and an enhancement in the cooling capacity of 22.5 %. The 22.4 % increase in coefficient of performance would result in a decrease of energy consumption along a reduction of the greenhouse gases emissions. The proposed combination of a thermoelectric subcooler and an internal heat exchanger outperforms each of the technologies on their own and presents itself as a great controllable solution to boost the performance and reduce the greenhouse gasses emissions of transcritical carbon dioxide refrigeration cycles.

1. Introduction

The Physical Science Basis report from The Intergovernmental Panel on Climate Change on 2021 describes thoroughly how climate change and extreme events can be attributed to the build-up of anthropogenic greenhouse gas (GHG) emissions in the atmosphere [1]. The report, described as a code red for humanity by the United Nations Secretary-General, states that unless immediate, rapid and large-scale reductions in GHG emissions occur, global warming will surpass 2 °C by 2100 [2]. The refrigeration sector, including air conditioning, heat pumps and cryogenics, consumes 20 % of the global electricity [3], is responsible for 7.8 % of the global GHG emissions and the energy consumption of the sector is expected to more than double by 2050 [4]. These data remark the impact of the refrigeration sector and its importance in confronting global warming in the future decades. The emissions of the sector are divided in two terms, direct and indirect, and to properly diminish the effect of the sector in global warming, important reductions need to be achieved in both terms. The direct emissions are related to the leakage of hydrofluorocarbon (HFC) refrigerants (37 %) while the indirect emissions are linked to the electricity needed to operate the systems (63 %) [3].

Ratified by more than 120 countries, the Kigali Amendment to the Montreal Protocol of 2016 focuses on reducing the direct emissions of the refrigeration sector by limiting the production and use of HFC refrigerants [5]. The fulfilment of the amendment would allow to avoid an increase in global warming between 0.1 °C to 0.3 °C by the end of the century [4]. Nowadays, multiple regulations leaded by the F-Gas Directive from the European Union, restrict or ban the use of HFC fluids in refrigeration systems [6]. As a consequence, the use of natural refrigerants such as carbon dioxide (CO_2) with almost negligible direct emissions has risen in popularity during the past few decades.

* Corresponding author.
E-mail address: miguel.araiz@unavarra.es (M. Araiz).

https://doi.org/10.1016/j.enconman.2022.115963
Received 15 March 2022; Received in revised form 11 June 2022; Accepted 2 July 2022
Available online 19 July 2022

Nomenclature

Variables

COP	Coefficient of performance
c_p	Specific heat capacity at constant pressure ($J\,kg^{-1}\,K^{-1}$)
h	Enthalpy ($kJ\,kg^{-1}$)
$\dot{m}$	Mass flow rate ($kg\,h^{-1}$)
N^{o}	Number (#)
P	Pressure (bar)
$\dot{Q}$	Heat flux (W)
q	Specific cooling capacity ($kJ\,kg^{-1}$)
RH	Relative humidity (%)
Sub	Subcooling (K)
T	Temperature (°C)
$\dot{V}$	Volumetric flow rate ($m^3\,h^{-1}$)
$\dot{W}$	Power consumption (W)
Δ	Difference
ρ	Density ($kg\,m^{-3}$)

Subscripts and superscripts

amb	Ambient
$base$	Base cycle
$block$	Subcooling block
CO_2	Carbon dioxide
$cold$	Cold face/side
$comp$	Compressor
$crit$	Critical point
$evap$	Evaporator
gc	Gas-cooler
gly	Water + glycol mixture
hot	Hot face/side
IHX	Internal heat exchanger
N	Thermoelectric subcooling block N
opt	Optimal/optimum
TEM	Thermoelectric module
$TEMs$	Thermoelectric modules
$TESC$	Thermoelectric subcooler
tot	Total

Other abbreviations and acronyms

DAQ	Data acquisition system
GHG	Greenhouse gas/gases
GWP	Global warming potential
HFC	Hydrofluorocarbon
HX	Heat exchanger
ODP	Ozone depletion potential

Although the direct emissions produced by CO_2 refrigeration systems are virtually null, the indirect emissions related to the electric consumption are still present and need to be properly addressed. The use of CO_2 as a refrigerant for vapour compression refrigeration facilities was presented by professor Gustav Lorentzen in 1995 as an alternative to artificial refrigerants due to its excellent properties [7]. CO_2 is a non-flammable, non-toxic refrigerant with zero Ozone Depletion Potential (ODP) and an almost negligible direct Global Warming Potential (GWP). As a consequence of its low critical temperature ($T_{Crit\ CO_2}$ = 30.89 °C), CO_2 vapour compression plants are forced to work under transcritical conditions when ambient temperature surpass a certain threshold. The transcritical thermodynamic cycle, due to exergy losses, results in lower coefficients of performance of the facility and therefore, an increase in its energy consumption [8]. In countries with high ambient temperatures, like the south of Europe, the lower coefficient of performance (COP) of the transcritical CO_2 refrigeration cycle makes it less environmentally friendly, as the increase in energy consumption also results in an increase in indirect GHG emissions.

In order to decrease the energy consumption of transcritical CO_2 refrigeration facilities and consequently, reduce the indirect GHG emissions of these refrigeration plants, many technologies have been the focus of recent studies to improve the performance of CO_2 transcritical vapour compression cycles. For high power installations the most studied and successful solutions are the following. Zhu et al. [9] performed an experimental investigation of a transcritical CO_2 vapour compression refrigeration facility and reported a maximum improvement in the COP of 11.3 % by utilizing an ejector and optimizing its mass balance. Llopis et al. [10] evaluated the effect of including a dedicated mechanical subcooling that used R1234yf as a refrigerant in a transcritical CO_2 refrigeration system, the results reported an experimental enhancement in the COP of 30.3 %. Sanchez et al. [11], evaluated a mechanical subcooling system that used R600a and an internal heat exchanger to boost the performance of a transcritical CO_2 vapour compression system, the enhancement of the COP obtained with the mechanical subcooler was of the 16.1 % while the boost with the internal heat exchanger was of the 6.2 %. Through a theoretical study, Sarkar et al. [12] analysed the optimum configuration for a parallel compression transcritical CO_2 vapour compression cycle, the author reported computational data with a maximum enhancement in the COP of 47.3 % for the studied range. Chesi et al. [13] performed a computational and experimental analysis in a transcritical CO_2 parallel compression cycle. The computational results by Chesi et al. reported a maximum enhancement in the COP of 30 % and regarding the experimental enhancements obtained the author concludes that the values were lower than the computational ones. Megdouli et al. [14] proposed a novel enhanced transcritical CO_2 refrigeration cycle for power and cold generation, the configuration includes two compressors, a gas-cooler, a condenser, a recirculation pump, an eyector, two evaporators and a turbine generator. The proposed configuration was theoretically modelled and the results reported by Megdouli show an enhancement between the 50 % to 110 % when producing cold and heat. Catalán-Gil et al. [15] through a theoretical analysis studied the effect of two-stage CO_2 systems to boost the performance while covering the demand at two different thermal levels for a medium size supermarket. Catalan stated that the basic booster with economizer and additional compression stage reported the highest reduction in the annual energy consumption between 3.5 % to 8.5 % in different European cities. Although these solutions for high power systems improve the performance of the refrigeration facility, they are not well suited for low–medium power due to the increase in complexity of the system, the inclusion of several compressors, or the high economical cost. For this low–medium power range, two technologies have been proven as viable solutions to increase the COP of transcritical CO_2 refrigeration systems: the thermoelectric subcooler (TESC) and the internal heat exchanger (IHX).

A thermoelectric subcooler (TESC) is based on the use of thermoelectric modules (TEMs). Thanks to the Peltier effect, the TEMs are able to force a heat flux using electrical power [16]. The TESC is located at the outlet of the gas-cooler and subcools the refrigerant before the expansion process. The main effect of this technology is an increase in the specific cooling capacity that, if properly managed, compensates the extra electrical consumption of the TEMs and increases both the cooling capacity and the COP of the installation. The internal heat exchanger (IHX) is a simple and low cost solution that can improve the performance of vapour compression cycles significantly. It consists of a heat exchanger that allows a natural heat flux between the low pressure refrigerant at the outlet of the evaporator and the high pressure refrigerant at the outlet of the gas-cooler. The effect of the IHX is an increase in specific cooling capacity and specific compression work

that depending on the refrigerant, the dimensions of the heat exchanger or the working conditions of the cycle, can improve or worsen the performance of the refrigeration system. Both of these two technologies have been the focus of recent studies to boost the performance of transcritical CO_2 refrigeration systems by increasing the specific cooling capacity of the refrigeration cycle through a subcooling process at the outlet of the gas-cooler.

The inclusion of a TESC in combination with an ejector was theoretically analysed by Liu et al. in 2019 [17] for a transcritical CO_2 vapour compression cycle, reporting theoretical improvements in the COP of 39.34 %. When including a TESC in an experimental facility, Sanchez et al. [18] reported improvements in the COP of a transcritical CO_2 refrigeration system of 9.9 %. Aranguren et al. [19] in the most recent study on an experimental transcritical CO_2 refrigeration plant with a TESC, reported improvements in the cooling capacity and the COP of 15.3 % and 11.3 % respectively. Regarding internal heat exchangers, Torrella et al. [20] reported experimental improvements in the COP of a transcritical CO_2 refrigeration facility of 12 % through the inclusion of an IHX. Sanchez et al. [21] managed to obtain an enhancement in the COP of 13 % using two IHXs in a transcritical CO_2 refrigeration plant.

Regarding the combination of an internal heat exchanger and thermoelectricity, the only study in the literature was performed by Kwan et al. [22]. The proposed solution consisted of an internal heat exchanger with thermoelectric modules working in cooling mode to boost the effect or the IHX or in generation mode to take advantage of the heat flux at the internal heat exchanger. The theoretical study concluded that the thermoelectric generation internal heat exchanger enhanced the COP of the facility by 5 % while the IHX assisted with the thermoelectric modules reduced the performance of the cycle. It is worth to remark that the analysis by Kwan et al. theoretically studied an internal heat exchanger integrated with thermoelectric modules and not the proposed solution on this work: a combined solution of an internal heat exchanger and a thermoelectric subcooling system to boost the performance of a transcritical CO_2 vapour compression refrigeration facility.

The inclusion of a TESC or an IHX has been proven as a viable solution to boost the performance of transcritical CO_2 refrigeration cycles. However, the two technologies have always been tested separately and the combination of a TESC and an IHX in a facility is yet to be explored. Neither theoretical or experimental research is present in the literature regarding the combination of a TESC and an IHX for a vapour compression refrigeration facility. In this context, the authors propose the novel combination of a TESC and an IHX working together to boost the performance of a transcritical CO_2 vapour compression refrigeration system. The combination of these two technologies could produce even greater enhancements in the COP and cooling capacity of a transcritical CO_2 refrigeration cycles, reducing their energy consumption and therefore, diminishing the indirect GHG emissions that they produce.

This paper presents, for the first time, the combination of a thermoelectric subcooler (TESC) and an internal heat exchanger (IHX) for an experimental transcritical CO_2 refrigeration facility. The TESC, being a controllable and polyvalent system, is first analysed to comprehend its working principles and understand how to successfully combine it with the passive IHX in the transcritical CO_2 refrigeration cycle. The results show that the inclusion of the TESC at the outlet of the gas-cooler benefits the refrigeration system and therefore, the most suitable combination of the TESC and the IHX corresponds to include the TESC at the outlet of the gas-cooler and the IHX at the outlet of the TESC. After that, both systems are experimentally tested together to measure the improvements obtained with this combination of technologies in terms of cooling capacity and COP. In addition, the results obtained are compared with previous studies performed with each of the technologies. The experimental plant is described in Section 2 alongside the TESC, the IHX and the monitoring system. In Section 3 the methods followed during the experimental tests is described. Then, in Section 4, the results obtained through the tests are presented and discussed. Lastly, in Section 5 conclusions are drawn.

Table 1
Commercial reference of the main elements of the refrigeration plant.

Designation	Element	Commercial reference
A	Compressor	SANDEN SHR17
B	Oil filter	TECNAC SAC 0-130 bar
C	Gas-cooler	ECO TKE351A2R.1620
F	Coriolis flow meter	ROTAMASS NANO
G	Back-pressure valve	CAREL E2V05CS100
H	Refrigeration tank	TECNAC RV-10
I	Thermostatic valve	CAREL E2V05CS100
J	Evaporator	SWEP B18Hx10/1P-SC-U
K	Electromagnetic flow meter	AXG ADMAG TI

2. Experimental plant

In this section the experimental refrigeration plant is thoroughly described. The main elements and working principles of the transcritical vapour compression cycle are explained in Section 2.1. The TESC and the IHX are explained in Section 2.2 and Section 2.3, respectively. Lastly, the monitoring system is described in Section 2.4.

2.1. Refrigeration facility

Each of the main elements of the refrigeration facility is highlighted with a letter in the schematic of Fig. 1. Additionally, the numbers in the schematic refer to points of interest regarding the thermodynamic cycle. The refrigeration facility consists of a transcritical CO_2 vapour compression refrigeration cycle. It is provided with a two valve expansion system that allows the control of the pressure of the gas-cooler and the useful superheating at the evaporator at the same time. In addition, the facility is able to work under multiple configurations thanks to a bypass valve system that allows to connect and disconnect the thermoelectric subcooler (D) and the internal heat exchanger (E), which are described in detail in Section 2.2 and Section 2.3, respectively.

The system consists of: an hermetic compressor (A) that increases the pressure from the evaporation level to the gas-cooler pressure; a coalescent oil-filter (B) that separates the lubricant oil from the refrigerant and periodically returns it to the compressor; an air finned gas-cooler (C) where the heat from the refrigerant is rejected to the ambient; a coriolis flow meter (F) that measures the refrigerant mass flow rate that flows around the refrigeration facility; an electronic back-pressure valve (G) used to maintain the pressure level of the gas-cooler at a designated level; a tank (H) that accumulates CO_2 between the 2 electronic valves; an electronic thermostatic valve (I) used to maintain the useful superheating at the evaporator constant; a brazed plate evaporator (J) where the CO_2 evaporates at constant temperature while extracting heat from a secondary fluid; and lastly, an electromagnetic volumetric flow meter (K) that measures the volumetric flow rate of the secondary fluid. The commercial references of the main elements are collected in Table 1 and the experimental plant is shown in Fig. 2.

The secondary fluid consists of a water–glycol mixture (40 % glycol) that is heated up in a controlled closed-loop circuit using an electrical cartridge. In addition, the facility also includes secondary safety elements that do no impact the thermodynamic cycle such as access valves, security valves, filters, etc. Lastly, all the elements are connected using copper K65 pipes and are insulated with foam to minimize heat losses with the ambient.

2.2. Thermoelectric subcooler (TESC)

The main objective of the TESC is to increase the specific cooling capacity of the facility by subcooling the refrigerant at the outlet of the gas-cooler. For that, a TESC makes use of thermoelectric modules (TEMs) that taking advantage of the Peltier effect extract heat from the refrigerant. The TESC presented in this work is subdivided in 4 identical subcooling blocks, Fig. 3 shows an schematic of the complete

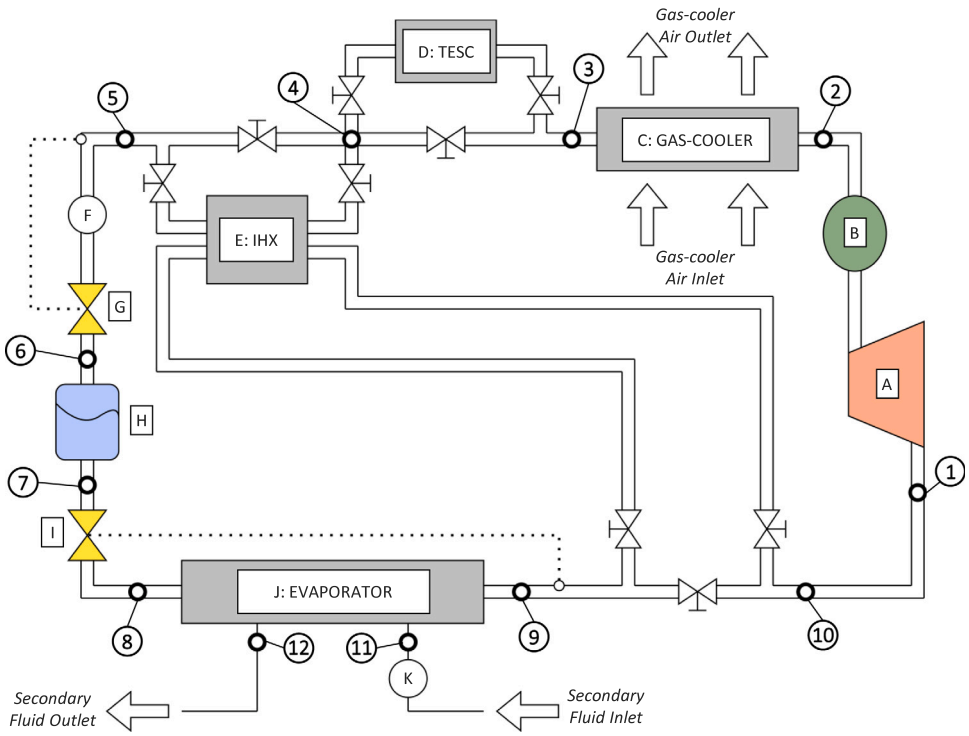

Fig. 1. Schematic of the refrigeration facility with the main elements and thermodynamic points of interest.

Fig. 2. Experimental vapour compression refrigeration plant.

subcooler with the 4 subcooling blocks. Each of the subcooling blocks consists of 2 cold side heat exchangers, 4 TEMs, and 4 hot side heat exchangers. Taking advantage of a bypass valve system the subcooler is able to work with 1, 2, 3 or 4 of the thermoelectric blocks at the same time, which corresponds to 4, 8, 12 and 16 TEMs, respectively. A detailed schematic of a block of the TESC is presented in Fig. 4 where each element can be clearly identified. The cold side heat exchangers (CO_2 HX) are represented in blue colour, the TEMs are highlighted in green, and the hot side heat exchangers (Ambient HX) are represented in red colour.

The refrigerant enters the subcooling block and passes through the cold side heat exchangers. The cold side heat exchangers are self built and each of them consists of a copper block of 56 × 56 × 12 mm^3 in which an internal channel for the CO_2 has been mechanized. The length of the inner circuit is 336 mm with a circular cross section of 3 mm of diameter. The cold side heat exchanger is provided with 2 planar surfaces where the cold face of 2 TEMs are placed. The TEMs used in the system are commercial modules manufactured by Marlow Industries (RC12-6L) with 2 planar surfaces of 40 × 40 mm^2, 127 thermocouples and a thickness of 3.9 mm. A thermoelectric module (TEM) is a solid state refrigerator that when supplied with an electrical current produces an increase in the temperature of its hot face and a decrease the temperature of its cold face via the Peltier effect. This thermal gradient between the faces of the TEM forces a heat flux that goes from the cold face to the hot one. As stated before, the cold faces of the TEMs are placed in contact with the heat exchangers of the cold side, in order to extract heat from the refrigerant and increase the specific cooling capacity of the cycle. The hot side heat exchangers are commercial heat pipe heat exchangers with fins fabricated by Xigmatek (Xigmatek HDT-S983 Nepartak). They are placed in contact with the hot face of the TEMs and are used to reject heat into the ambient. The heat exchangers are attached with 6 mm screws between each others to secure the subcooler. In addition, 4 low consumption fans are used to circulate air through the fins of the hot side heat exchangers. Lastly, graphite sheets are located at both faces of the TEMs as interface material to reduce the contact thermal resistances and increase the performance of the TEMs.

The fundamental working principles of the TESC are the following: refrigerant gets in and flows across the cold side heat exchangers while heat is extracted from the refrigerant ($\dot{Q}_{CO_2}$); the heat flux is forced by the electrical power supplied to the TEMs ($\dot{W}_{TEM}$) thanks to the Peltier effect; lastly, heat is rejected into the ambient ($\dot{Q}_{amb}$) by the heat exchangers of the hot side. The heat and power fluxes are properly highlighted in the schematic of Fig. 4, which represents one of the 4 identical blocks of the TESC. As the refrigerant passes across of the

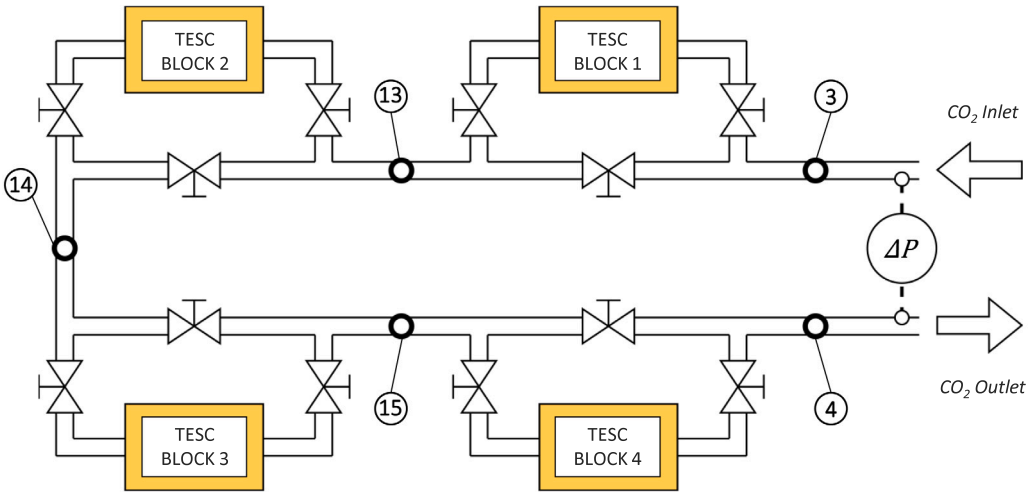

Fig. 3. Schematic of the thermoelectric subcooler (TESC).

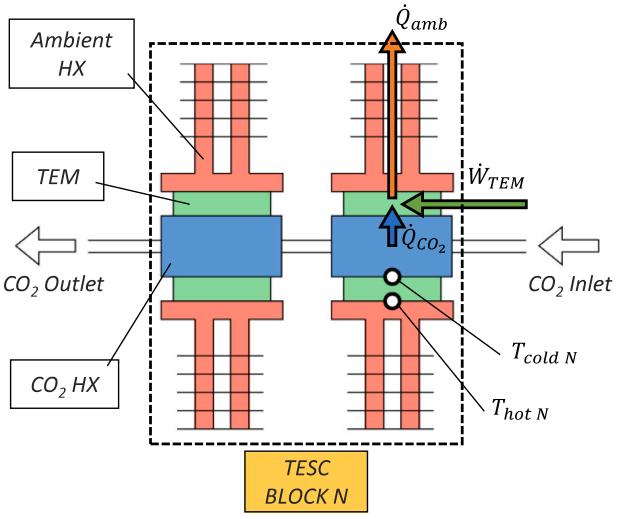

Fig. 4. Schematic of one block of the thermoelectric subcooler (TESC).

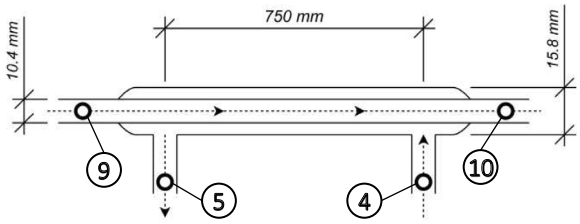

Fig. 5. Schematic of the internal heat exchanger (IHX).

Table 2
Main characteristics of the measurement equipment.

Measuring device	Unit	Accuracy
Thermocouple T	°C	±0.5 °C
Pressure gauge	bar	±0.25 % of full scale
Differential pressure sensor	bar	±0.055 % of reading
Voltmeter	V	±0.5 % of reading
Hall effect sensor	A	±0.2 % of reading
Network analyser	W	±0.5 % of reading
Hygrometer	%	±2 %
Electromagnetic volumetric meter	$m^3\ h^{-1}$	±0.3 % of reading
Coriolis flow meter	$kg\ h^{-1}$	±0.2 % of reading

subcooler, its temperature decreases gradually, increasing the specific cooling capacity at the evaporator and introducing the power supplied to the TEMs as another consumption of the system. If properly designed and operated, the increase in specific cooling capacity compensates the extra consumption of the TEMs and as a consequence, the COP and cooling capacity of the system are enhanced.

2.3. Internal heat exchanger (IHX)

The main objective of the IHX is to produce a subcooling at the outlet of the gas-cooler in order to increase the specific cooling capacity of the system. The IHX presented in this work consists of a concentric tube heat exchanger built in stainless steal. The internal diameter of the inner pipe is 10.4 mm with a thickness of 1.7 mm and the internal diameter of the outer pipe is 15.8 mm with a thickness of 2.8 mm. The total length of the heat exchanger is 800 mm with an effective heat exchange length of 750 mm. An schematic of the heat exchanger with the main dimensions is shown in Fig. 5.

The high pressure refrigerant at the outlet of the gas-cooler flows through the outer channel and the low pressure refrigerant from the outlet of the evaporator flows in counter flow configuration across the inner channel. A natural heat flow appears at the heat exchanger, subcooling the refrigerant at the outlet of the gas-cooler and increasing the temperature at the outlet of the evaporator. This produces an increase in the specific cooling capacity and an increment in the specific compression work at the compressor. In a transcritical CO_2 refrigeration cycle the enhancement of the cooling capacity compensates the increase in compression work and as a consequence the COP of the refrigeration facility and the cooling capacity are enhanced.

2.4. Monitoring system

The experimental plant is monitored using temperature thermocouples, pressure gauges, a pressure difference probe, voltmeters, hall effect sensors, a network analyser, an hygrometer, a volumetric flow meter and a mass flow meter. The main characteristic of the measuring equipment are collected in Table 2.

Thermocouples are located to monitor temperature across the refrigeration facility from points 1 to 10, covering the most important

states of the thermodynamic cycle. Points 11 and 12, that correspond to the inlet and outlet of the secondary fluid into the evaporator, are monitored using immersion thermocouples. Temperature probes are used between the blocks of the TESC in points 13, 14 and 15 to measure the subcooling produced alongside the subcooler. In addition, the temperature of both faces of one TEM in each subcooling block ($T_{cold\ N}$ and $T_{hot\ N}$, highlighted in Fig. 4) are monitored to calculate the temperature difference between the faces of the TEMs. The last temperature sensors are located in the climatic chamber to monitor ambient temperature. Pressure gauges are located in points 1, 2, 3, 5, 6 and 8 of the refrigeration facility. Also, a differential pressure sensor measures the pressure drop produced in the TESC between points 3 and 4 of the thermodynamic cycle. The direct current and voltage supplied to each block of the TESC is monitored using a digital voltmeter and a hall effect sensor. A network analyser measures the power consumption of the compressor. The humidity of the air inside the climatic chamber is monitored using an hygrometer. The volumetric flow rate of the secondary fluid (water + glycol mixture) is measured with an electromagnetic flow meter before entering the evaporator. And lastly, the mass flow rate of CO_2 is monitored using a coriolis mass flow meter located at the inlet of the back pressure valve. The location of the mentioned points can be clearly appreciated in Figs. 1, 3, 4 and 5.

To capture all the measurements a data acquisition system (DAQ) from National Instruments is used. The DAQ is connected to a personal computer using Labview and the data are stored and treated utilizing Microsoft Excel. Lastly, to calculate the properties of the CO_2 and the water + glycol mixture, Refprop v.10 and SecCool v1.33 are used.

3. Methods

The refrigeration facility is tested inside a climatic chamber where ambient temperature and humidity are controlled. During the experimental tests the refrigeration facility operates until steady state conditions are achieved and then data is collected during 20 min of continuous operation. The conditions at which the analysis of the TESC is performed are collected in Section 3.1 and the conditions at which the combination of the TESC and IHX is tested are described in Section 3.2.

3.1. Conditions for the analysis of the TESC

To analyse the working principles of the TESC the refrigeration cycle is tested at climatic class 3 conditions, ambient temperature (T_{amb}) at 25 °C and ambient relative humidity (RH_{amb}) of 60 %, with an evaporation temperature (T_{evap}) of −10 °C. The evaporation temperature is controlled with the auxiliary system and ambient conditions are controlled using the climatic chamber. The TESC is tested with 1, 2, 3 and 4 subcooling blocks, which corresponds to 4, 8, 12 and 16 TEMs, respectively. In addition, it includes a controllable variable on the form of the voltage supplied to the TEMs which impacts the performance of the system. For that, the voltage supplied to the TEMs is varied from 0.5 to 6 V to obtain the optimum operation voltage for each case. Lastly, the system is tested for different gas-cooler pressures to obtain optimum working conditions for each configuration. Is worth to remark the importance of analysing the number of TEMs and the voltage supplied to the them to optimize the performance of the TESC.

3.2. Conditions for the cycle with the TESC and the IHX

The refrigeration cycle with the TESC and the IHX are tested at climatic class 3, 4 and 7. The evaporation level (T_{evap}), ambient temperature (T_{amb}) and ambient relative humidity (RH_{amb}) are collected for each climatic class in Table 3. For all the tests performed with the TESC in combination with the IHX, all 4 blocks of the subcooler (16 TEMs) are utilized. Lastly, different gas-cooler pressures and voltages supplied to the TEMs are tested to achieve optimum working conditions of the combined system.

Table 3
Climatic class 3, 4 and 7 conditions.

Climatic class	Label for graphs	T_{evap} (°C)	T_{amb} (°C)	RH_{amb} (%)
3	CC3	−10	25	60
4	CC4	−10	30	55
7	CC7	−10	35	75

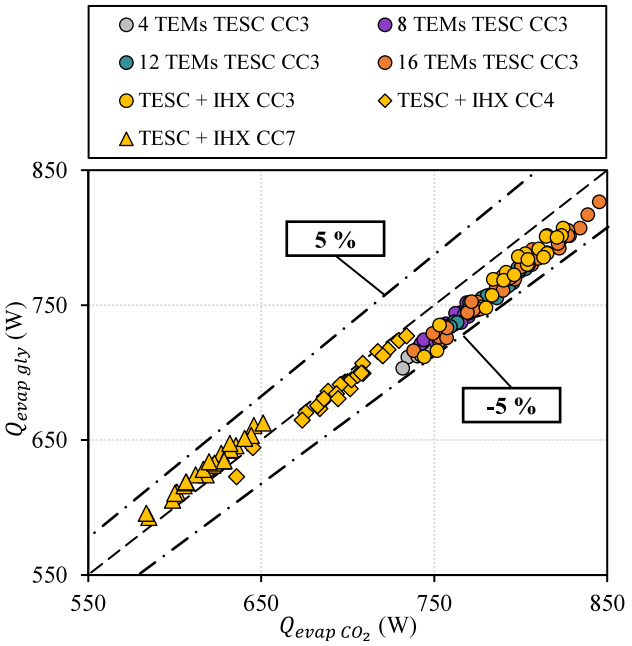

Fig. 6. Comparative of the calculated cooling capacity of the system between data collected from the refrigeration cycle and data from the auxiliary system.

3.3. Experimental data validation

In order to probe the reliability of the experimental methodology the cooling capacity of the refrigeration facility is compared between data collected with the refrigeration cycle and data collected with the auxiliary system. For that, Eqs. (1) and (2) are used to calculated the cooling capacity of the system and the comparative is presented in Fig. 6. Regarding Eq. (1), the mass flow rate of the CO_2 is obtained with the coriolis flow meter and the enthalpies of points 8 and 9 are obtained using their thermodynamic properties using Refprop v.10. In regard with Eq. (2), the volumetric mass flow rate of the water + glycol mixture is measured with the electromagnetic flow meter, the density and specific heat capacity are obtained through SecCool v1.33, and lastly, the temperature of points 11 and 12 are collected with T type thermocouples.

$$\dot{Q}_{evap\ CO_2} = \dot{m}_{CO_2} \cdot (h_9 - h_8) \tag{1}$$

$$\dot{Q}_{evap\ gly} = \dot{V}_{gly} \cdot \rho_{gly} \cdot c_{p\ gly} \cdot (T_{11} - T_{12}) \tag{2}$$

The comparative graph of Fig. 6 clearly shows a great agreement between the calculations performed with data from the refrigeration cycle and the auxiliary cycle which proves the consistency of the methodology. The data collected during the analysis of the TESC at climatic class 3 conditions are labelled: 4 TEMs TESC CC3, 8 TEMs TESC CC3, 12 TEMs TESC CC3 and 16 TEMs TESC CC3, which correspond to 1, 2, 3 and 4 subcooling blocks, respectively. The tests performed with the TESC + IHX correspond to TESC + IHX CC3, TESC + IHX CC4 and TESC + IHX CC7, for climatic class conditions 3, 4 and 7, respectively. The good agreement of the data, with deviations always between the ±5 % interval, proves the reliability and consistency of the followed methodology during the experimental tests.

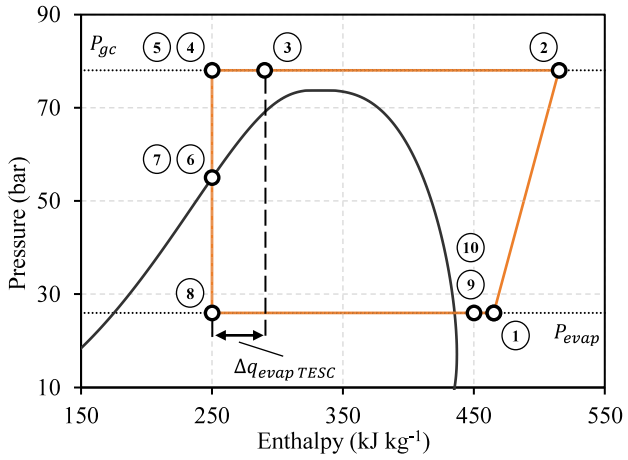

Fig. 7. Pressure vs Enthalpy diagram for the transcritical CO_2 cycle with TESC.

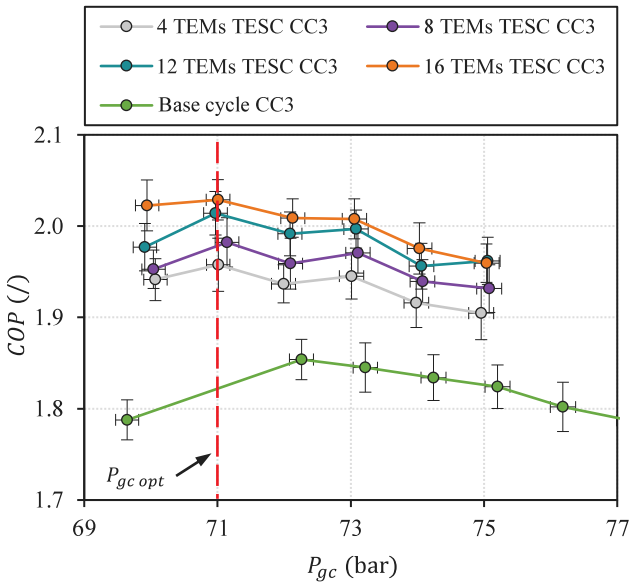

Fig. 8. COP vs P_{gc} for the transcritical cycle with TESC using 4, 8, 12 and 16 TEMs (V_{TEM} = 2 V) and the base transcritical cycle at climatic class 3 conditions.

4. Results and discussion

The results obtained with the TESC are analysed in Section 4.1 in regard of the COP of the refrigeration system, the cooling capacity and the performance of the subcooler. The results for the novel combination of TESC + IHX for a transcritical CO_2 refrigeration facility are presented in Section 4.2. In addition, the results are compared with previous studies performed with the same methodology for the base transcritical CO_2 refrigeration cycle, the transcritical CO_2 refrigeration cycle with the TESC and the transcritical CO_2 refrigeration cycle with the IHX.

4.1. Analysis of the thermoelectric subcooler (TESC)

In this section the performance of the TESC as part of the refrigeration facility is analysed. For that, the subcooler is tested with 4, 8, 12 and 16 TEMs (1, 2, 3 and 4 subcooling blocks, respectively) for different gas-cooler pressures and different voltages supplied to the TEMs at climatic class 3. A sample pressure vs enthalpy diagram of the transcritical CO_2 cycle with TESC is presented in Fig. 7

4.1.1. Optimum gas-cooler pressure

The effect that the TESC has on the COP of the refrigeration facility is analysed in Fig. 8 as a function of the pressure of the gas-cooler for 4, 8, 12 and 16 TEMs while supplied with 2 V. In addition, the COP of the base cycle as a function of the pressure of the gas-cooler is plotted for comparison. The COP of the refrigeration facility is calculated using Eq. (3) and the percentage improvements obtained for the COP and the cooling capacity are calculated in comparison with the optimum base cycle using Eq. (4) where X is either the COP or the cooling capacity.

$$COP = \frac{\dot{Q}_{evap}}{\dot{W}_{tot}} = \frac{\dot{Q}_{evap}}{\dot{W}_{comp} + \dot{W}_{TEMs}} \tag{3}$$

$$\Delta X = \frac{X - X_{base}}{X_{base}} \cdot 100 \tag{4}$$

The optimum gas-cooler pressure for climatic class 3 conditions with the TESC remains constant around 71.0 bar for 4, 8, 12 and 16 TEMs. At this pressure, including the TESC improves the COP of the refrigeration facility in comparison with the base cycle by 5.6 % with 4 TEMs, 6.3 % with 8 TEMs, 8.5 % with 12 TEMs and 9.4 % with 16 TEMs. The values are obtained with a voltage supplied to the TEMs of 2.0 V, the effect of the voltage supplied to the TEMs is explained in detail in Section 4.1.2. Regarding the cooling capacity of the facility, adding the TESC reports enhancements at optimum operation conditions of 5.1, 7.3, 11.0 and 14.1 % with 4, 8, 12 and 16 TEMs at 2 V, respectively.

4.1.2. Optimum voltage supplied to the TEMs

The voltage supplied to the TEMs has a critical impact in the performance of the subcooler and the whole refrigeration cycle. Fig. 9 depicts the percentage variations of the cooling capacity, the power consumption and the COP of the facility in comparison with the base cycle as a function of the voltage supplied to the TEMs. The data presented in Fig. 9 corresponds to the optimum gas-cooler pressure of 71.0 bar for climatic class 3 conditions and 16 TEMs. The percentage variations obtained for the power consumption in comparison with the base cycle are obtained using Eq. (4) where X is the power consumption.

As the voltage supplied to the TEMs increases, the cooling capacity of the refrigeration facility is enhanced in an almost linear manner. For higher voltages the power consumption of the facility rapidly increases which turns into a lower COP of the facility.

The graph of Fig. 9 clearly depicts that an optimum value for the COP of the facility is obtained between 1.5 and 2.0 V supplied to the TEMs. Still, for higher voltages the COP rapidly drops due to the high increase in consumption of the TEMs. The difference in COP between 1.5 to 2.0 V supplied to the TEMs is almost negligible and thus, both working points would be close to optimal regarding the COP of the system. However, in regard with the cooling capabilities of the system, working at higher voltages presents clear advantages in cooling capacity. Supplying the TEMs with 1.5 V corresponds to an increase in COP of 9.3 % and an increase in cooling capacity of 11.0 %, whereas supplying the TEMs with 2.0 V corresponds to an almost identical enhancement in the COP of 9.4 % and a larger increase in cooling capacity of 14.1 %. Therefore, working with 2.0 V presents greater benefits than with 1.5 V. This effect is also present when working with 4, 8 and 12 TEMs as it can be properly appreciated in Table 4, where the COP remains close for 1.5 and 2.0 V but starts decreasing for 2.5 V.

The table collects the data for 4, 8, 12 an 16 TEMs at an optimum gas-cooler pressure of 71.0 bar and a voltage supplied to the TEMs of 1.5, 2.0 and 2.5 V. The following parameters are collected in Table 4: cycle configuration, optimum gas-cooler pressure, voltage supplied to the TEMs, COP of the TEMs, power consumption of the compressor, power consumption of the TEMs, total power consumption, subcooling produced with the TESC, pressure drop at the TESC, cooling capacity at the evaporator, increase in cooling capacity in comparison with the base cycle, COP of the cycle and improvements in the COP in

Table 4
Results for the transcritical cycle with TESC using 4, 8, 12 and 16 TEMs and the base cycle at climatic class 3 conditions.

Cycle configuration	$P_{gc\ opt}$ (bar)	V_{TEMs} (V)	COP_{TEMs} (/)	$\dot{W}_{comp}$ (W)	$\dot{W}_{TEMs}$ (W)	$\dot{W}_{tot}$ (W)	Sub (K)	ΔP_{TESC} (mbar)	$\dot{Q}_{evap}$ (W)	$\Delta\dot{Q}_{evap}$ (%)	COP (/)	ΔCOP (%)
Base cycle	72.3	–	–	385.0	–	385.0	–	–	713.7	–	1.85	–
TESC with 4 TEMs	71.0	1.5	7.2	376.7	3.4	380.1	1.2	119	742.8	4.1	1.95	5.4
	71.0	2.0	5.2	377.3	5.9	383.3	1.6	119	750.3	5.1	1.96	5.6
	71.0	2.5	4.0	376.2	9.2	385.4	1.9	118	751.1	5.2	1.95	5.1
TESC with 8 TEMs	71.1	1.5	6.6	376.8	6.4	383.2	2.3	217	756.7	6.0	1.97	6.5
	71.1	2.0	4.7	377.4	11.4	388.8	3.0	214	766.2	7.3	1.97	6.3
	71.1	2.5	3.7	377.5	17.6	395.1	3.6	212	767.2	7.5	1.94	4.8
TESC with 12 TEMs	71.0	1.5	6.5	376.5	9.6	386.1	3.5	324	777.6	8.9	2.01	8.6
	71.0	2.0	4.7	376.8	17.0	393.8	4.5	321	792.2	11.0	2.01	8.5
	70.9	2.5	3.6	377.7	26.3	404.0	5.7	313	798.2	11.8	1.98	6.6
TESC with 16 TEMs	71.0	1.5	6.3	378.1	12.7	390.8	4.6	411	792.3	11.0	2.03	9.3
	71.0	2.0	4.5	379.1	22.4	401.4	6.1	396	814.5	14.1	2.03	9.4
	70.9	2.5	3.4	377.6	34.7	412.3	7.6	402	828.1	16.0	2.01	8.3

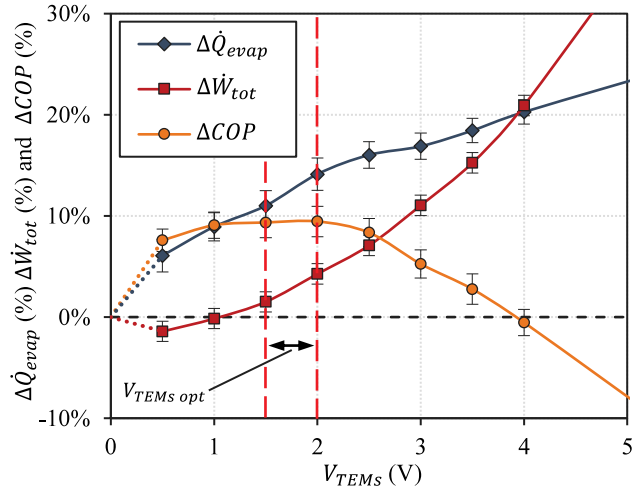

Fig. 9. Percentage variations in the cooling capacity, power consumption and COP with the TESC as a function of the voltage supplied to the TEMs for 16 TEMs, 71.0 bar and climatic class 3 conditions.

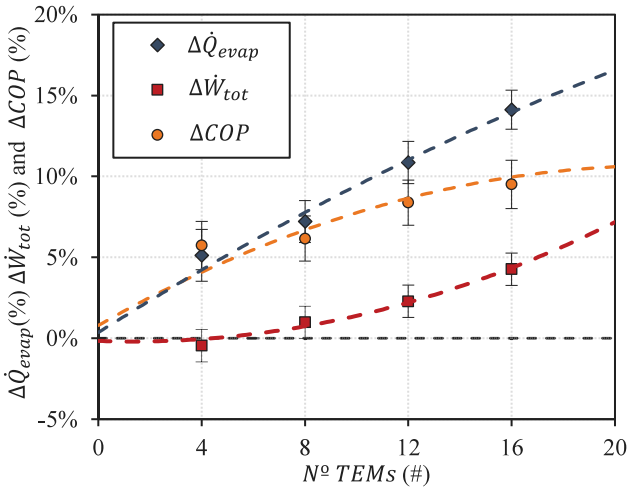

Fig. 10. Percentage variations in the cooling capacity, power consumption and COP with the TESC as a function of the number of TEMs for 2.0 V supplied to the TEMs, 71.0 bar and climatic class 3 conditions.

comparison with the base cycle. The COP of the TEMs is calculated by dividing the total heat extracted from the CO_2 in all the blocks of the TESC by the total power consumption of the TEMs in all the blocks of the TESC as in Eq. (5).

$$COP_{TEMs} = \frac{\dot{Q}_{CO_2\ TESC}}{\dot{W}_{TEMs}} \tag{5}$$

4.1.3. Optimum number of TEMs

From the data obtained during the tests is clear to conclude that the TESC performs better with 16 TEMs than any other of the cases tested. The transcritical CO_2 refrigeration cycle working with 16 TEMs in the TESC outperforms the base cycle in COP by 9.4 % and in cooling capacity by 14.1 % at climatic class 3 conditions. The tendency of increasing the number of TEMs is studied in Fig. 10 where the percentage variations of the cooling capacity, the power consumption and the COP of the facility in comparison with the optimum base cycle are represented as a function of the numbers of TEMs. The data corresponds to 2.0 V supplied to the TEMs and 71.0 bar of pressure at the gas-cooler. In the graph, the increase in cooling capacity seems to increase almost linearly with the number of TEMs. The power consumption increases slowly when the number of TEMs is low but raises when that number of TEMs goes up. Regarding the COP, it increases at first but starts to flatten as the number of TEMs increases. The tendency of the experimental data suggests that the optimum number of TEMs might be higher than 16 TEMs for climatic class 3 conditions, voltage supplied to the TEMs of 2.0 V and 71.0 bar. However, it also depicts that as the number of TEMs increases, a further increase in the number of TEMs would result in smaller improvement in performance while increasing the size and cost of the subcooler.

4.1.4. COP of the TEMs in each block

The performance of the TEMs is analysed in each block of the subcooler at a gas-cooler pressure of 71.0 bar with the 4 blocks of the subcooler (4 TEMs each block). In Fig. 11 the COP of the TEMs in each block is represented for voltages supplied to the TEMs around to the optimum (1.5, 2.0 and 2.5 V). The COP of the TEMs in a certain block is calculated by dividing the heat extracted from the CO_2 in that block by the power consumption of the TEMs in that block as in Eq. (6). In addition, the measured temperature gradient between the faces of the TEMs are presented for each block in the secondary vertical axis.

$$COP_{TEMs\ block\ N} = \frac{\dot{Q}_{CO_2\ block\ N}}{\dot{W}_{TEMs\ block\ N}} \tag{6}$$

Results show that the COP of the TEMs is always considerably higher for the first block of the TESC and then decreases for the 2nd to the 4th block. This effect is directly related to the temperature gradient between the CO_2 and the ambient. For the first block the temperature

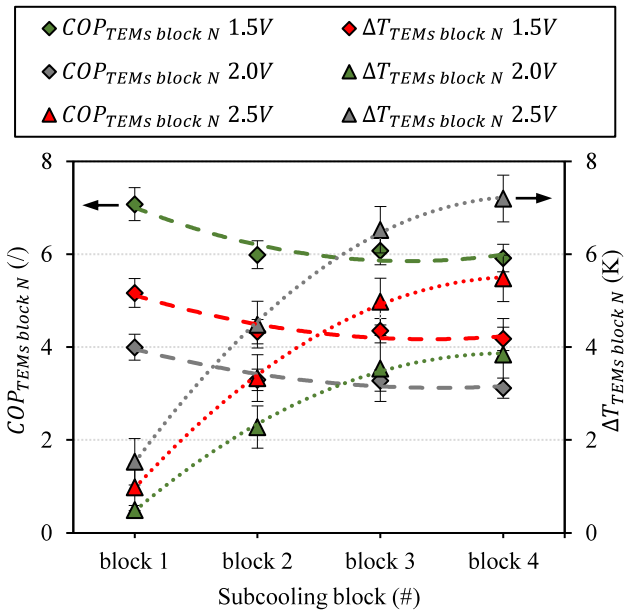

Fig. 11. COP of the TEMs for each subcooling block and temperature gradient between faces of the TEMs at each subcooling block for a gas-cooler pressure of 71.0 bar and a power supplied to the TEMs of 1.5, 2.0 and 2.5 V.

of the CO_2 is still higher than ambient temperature and therefore, the TEMs are working in the same direction the natural heat flux occurs. On the other side, for the rest of the blocks, the refrigerant is already subcooled below ambient temperature and therefore the subcooler is working against the natural heat flux, hence, the lower COP of the TEMs.

In order to increase the performance of the TESC in the combined system of TESC + IHX, the TESC should be the first subcooling system to operate to take advantage of this boosted performance of the TEMs at the beginning of the TESC. Therefore, to optimally boost the performance of the system for the combination of the TESC + IHX, the TESC should subcool the refrigerant at the outlet of the gas-cooler and the IHX should be located at the outlet of the TESC as in Fig. 1. The results for the combination of TESC + IHX are presented in Section 4.2.

4.1.5. Pressure drop at the TESC

The pressure drop at the TESC is collected in Table 4 when working with 4, 8, 12 an 16 TEMs. The pressure drop that occurs at the subcooler is negligible in comparison with the more than 70 bar of pressure of the gas-cooler. The average pressure drop measured with 4, 8, 12 and 16 TEMs is 119, 214, 319 and 405 mbar, respectively. This translates into a pressure drop between 100 to 120 mbar for each subcooling block of the TESC, which does not represent an issue in comparison with the high working pressures of the refrigeration facility.

4.2. Refrigeration cycle with the TESC + IHX

The combination of TESC + IHX is tested for climatic class 3, 4 and 7 conditions, different gas-cooler pressures and different voltages supplied to the TEMs. The TESC is included using the 4 subcooling blocks (16 TEMs) due to the greater increase in COP obtained during the analysis of the TESC. The results are compared with previous studies in which the refrigeration facility has been tested under the base transcritical CO_2 refrigeration cycle configuration, with only the TESC and with only the IHX. A sample pressure vs enthalpy diagram for the transcritical CO_2 refrigeration cycle with the combination of TESC + IHX is presented in Fig. 12.

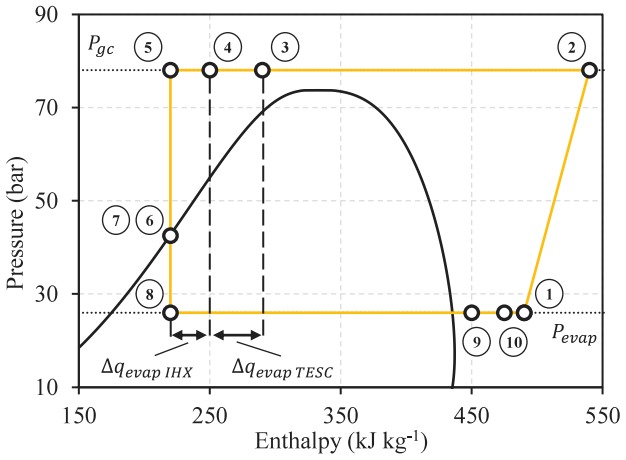

Fig. 12. Pressure vs Enthalpy diagram for the transcritical CO_2 cycle with TESC + IHX.

When using the TESC + IHX, the refrigerant at the outlet of the gas-cooler suffers 2 subcooling steps. First, the CO_2 is subcooled from point 3 to 4 by the TESC, taking advantage of the greater COP of the TEMs when working with low temperature differences between their faces. Secondly, the CO_2 gets subcooled from point 4 to 5 at the IHX while the natural heat flux heats the refrigerant from point 9 to 10 at the outlet of the evaporator. The combination of TESC + IHX produces a large subcooling effect on the refrigeration cycle that increases the specific cooling capacity of the system. At the same time, it also produces an increase in the specific compression work due to the reheating of the IHX and introduces the power consumption of the TEMs of the TESC. The experimental results show that the COP of the refrigeration facility increases and thus, the enhancement of specific cooling capacity surpasses the negative effects of the TESC and the IHX in the COP of the facility.

4.2.1. COP

In Fig. 13 the COP of the refrigeration facility is represented as a function of the pressure of the gas-cooler for the cycle with TESC + IHX. Graphs 13.a, 13.b and 13.c correspond to climatic class 3, 4 and 7 conditions, respectively. The results are compared with data for the base transcritical cycle, the cycle with IHX and the cycle with TESC from previous work [23]. The COP of the refrigeration facility is calculated using Eq. (3). Each represented point on Fig. 13 corresponds to the optimum voltage supplied to the TEMs that maximizes the COP of the facility for that gas-cooler pressure. Is worth to notice that the optimum COP of the refrigeration cycle with the TESC + IHX is obtained for low gas-cooler working pressures, close to the minimal working pressure at which the facility is able to work under stable conditions at transcritical state. As the gas-cooler pressure increases, the COP of the facility slowly decreases as depicted by Fig. 13. The maximum experimental COP obtained for the cycle with TESC + IHX is 2.10, 1.73 and 1.40 for climatic class 3, 4 and 7 conditions, respectively. In comparison with the base cycle, the TESC + IHX combination enhances the COP by 13.4 % for climatic class 3 conditions, 16.6 % for climatic class 4 conditions and 22.4 % for climatic class 7 conditions.

The results for the TESC + IHX are summarized in Table 5. The data collected in the table corresponds to the optimum gas-cooler pressure and voltage supplied to the TEMs that maximize the COP of the refrigeration facility. The table contains climatic class, cycle configuration, optimal gas-cooler pressure, variation of the optimum gas-cooler pressure in comparison with the base transcritical cycle, optimum voltage supplied to the TEMs, COP of the TEMs, subcooling

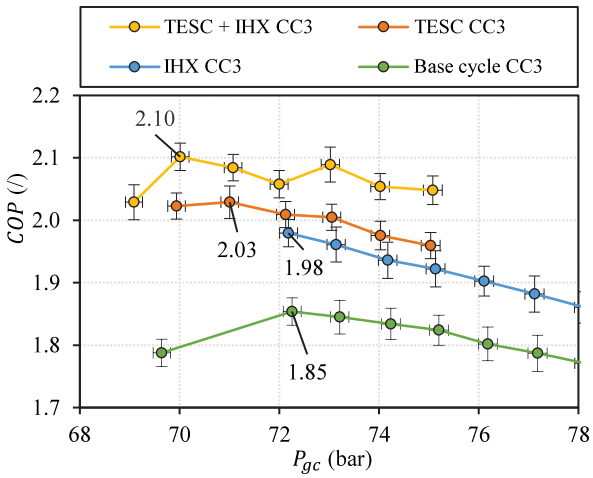

(13.a) COP vs P_{gc} for TESC + IHX, TESC, IHX and Base at CC3.

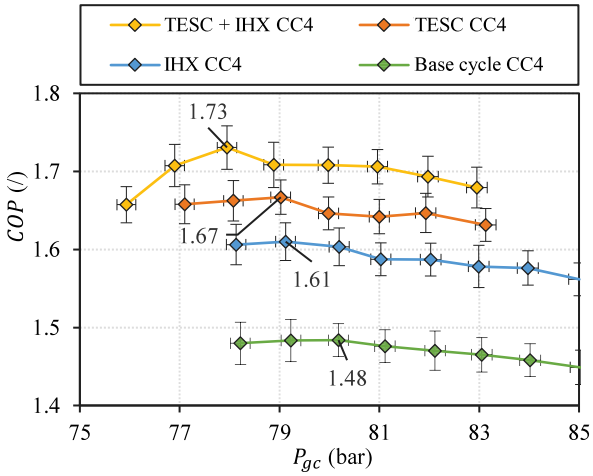

(13.b) COP vs P_{gc} for TESC + IHX, TESC, IHX and Base at CC4.

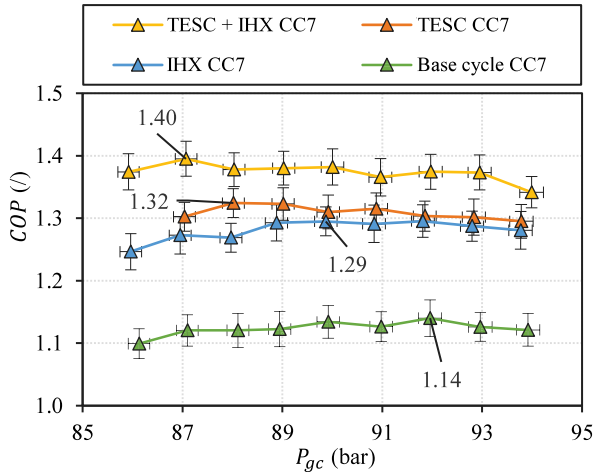

(13.c) COP vs P_{gc} for TESC + IHX, TESC, IHX and Base at CC7.

Fig. 13. COP vs P_{gc} for the TESC+IHX, TESC, IHX and Base cycle.

produced, power consumption of the compressor, power consumption of the TEMs, total power consumption, cooling capacity of the refrigeration facility, percentage improvement in the cooling capacity compared with the base cycle, COP of the refrigeration facility and percentage improvement in the COP compared with the base cycle.

As detailed by Table 5, the combination of a TESC + IHX outperforms by a large margin any of the two technologies on their own in terms of COP. These promising results remark that using simultaneously a TESC and an IHX in a transcritical CO_2 refrigeration cycle presents itself as a viable solution to boost the performance of vapour compression refrigeration systems.

4.2.2. Cooling capacity

The cooling capacity of the facility is obtained through Eq. (2) and the results are collected in Table 5 for the working conditions that maximize the COP of the facility. For all climatic class conditions, the TESC + IHX enhances the cooling capacity of the refrigeration facility in comparison with the base cycle. When maximizing the COP, the cooling capacity of the facility is improved in comparison with the base cycle by 12.6 % at climatic class 3 conditions, 16.9 % at climatic class 4 conditions and 22.5 % at climatic class 7 conditions.

It is worth to notice that the cooling capacity of the facility can be further increased when the TEMs are supplied with greater voltage while slightly decreasing the COP of the cycle. As an example, at climatic class 7, the optimum voltage supplied to the TEMs that maximizes the COP with the TESC + IHX is 2.0 V. At this conditions, the improvement in COP is 22.4 % and the enhancement in the cooling capacity is 22.5 %. However, when the voltage supplied to the TEMs is increased to 2.5 V (0.5 V more), the improvement in COP decreases slightly to 21.4 % but the cooling capacity rises to 24.4 %. This effect, already addressed with the TESC in Section 4.1.2, is also present with the TESC + IHX and shows the capability of the TESC to increase the cooling capacity of the system while working with a lower COP. This feature increases the flexibility of the refrigeration system with TESC + IHX and could result extremely relevant for the design of systems that need to match a certain cooling capacity for short periods of time during the year without over sizing the facility.

4.2.3. Gas-cooler pressure

The optimum gas-cooler pressure that maximize the COP of the installation decreases when using the TESC + IHX in comparison with the base cycle, only the IHX, or only the TESC. This effect is depicted in Fig. 13 and the differences in comparison with the base cycle in absolute values are collected in Table 5. The inclusion of the TESC + IHX reduces the optimum working pressure of the gas-cooler by 2.3 bar for climatic class 3 and 4 conditions and by 4.8 bar for climatic class 7 conditions. The optimum working pressure drop of the gas-cooler represents a beneficial feature for refrigeration facilities as the requirements for some components could be lower.

5. Conclusions

This work brings a novel experimental study of a transcritical carbon dioxide refrigeration facility that works simultaneously with a thermoelectric subcooler and an internal heat exchanger.

The performance of the thermoelectric subcooler is analysed in terms of coefficient of performance and cooling capacity at climatic class 3 conditions. The transcritical carbon dioxide refrigeration cycle working with the thermoelectric subcooler reports improvements in the coefficient of performance of 9.4 % and enhancements in the cooling capacity of 14.1 % for an optimum gas-cooler pressure of 71.0 bar and an optimum voltage supplied to the thermoelectric modules of 2.0 V. In addition, the analysis shows that the refrigeration facility benefits when using the thermoelectric subcooler directly at the outlet of the gas-cooler when the thermoelectric modules works in favour of the natural heat flux, resulting in a greater coefficient of performance of the modules.

The transcritical carbon dioxide refrigeration facility working simultaneously with the thermoelectric subcooler and the internal heat exchanger is tested at climatic class 3, 4 and 7 conditions. The results obtained report an increase in cooling capacity with the thermoelectric

Table 5
Results for the transcritical base CO_2 cycle, with IHX, with TESC and with TESC + IHX for CC3, CC4 and CC7.

Climatic class	Cycle configuration	$P_{gc\ opt}$ (bar)	$\Delta P_{gc\ opt}$ (bar)	$V_{TEMs\ opt}$ (V)	COP_{TEMs} (/)	Sub (K)	$\dot{W}_{comp}$ (W)	$\dot{W}_{TEMs}$ (W)	$\dot{W}_{tot}$ (W)	$\dot{Q}_{evap}$ (W)	$\Delta\dot{Q}_{evap}$ (%)	COP (/)	ΔCOP (%)
CC3	Base cycle	72.3	–	–	–	–	385.0	–	385.0	713.7	–	1.85	–
	IHX	72.2	−0.1	–	–	4.7	378.2	–	378.2	748.6	4.9	1.98	6.8
	TESC	71.0	−1.3	2	4.5	6.1	379.1	22.4	401.5	814.5	14.1	2.03	9.4
	TESC + IHX	70.0	−2.3	1.5	6.4	9.3	369.7	12.8	382.5	803.8	12.6	2.10	13.4
CC4	Base cycle	80.2	–	–	–	–	404.5	–	404.5	600.2	–	1.48	–
	IHX	79.2	−1.0	–	–	4.4	399.1	–	399.1	642.5	7.1	1.61	8.5
	TESC	79.0	−1.2	2	4.5	5.3	402.4	21.8	424.2	707.1	17.8	1.67	12.3
	TESC + IHX	77.9	−2.3	1.5	6.2	8.6	392.9	12.4	405.3	701.4	16.9	1.73	16.6
CC7	Base cycle	91.9	–	–	–	–	442.6	–	442.6	504.5	–	1.14	–
	IHX	89.9	−2.0	–	–	5.1	430.2	–	430.2	557.0	10.4	1.29	13.6
	TESC	88.0	−3.9	2.5	3.6	6.0	426.7	33.3	460.0	609.2	20.8	1.32	16.2
	TESC + IHX	87.1	−4.8	2	4.6	10.3	421.6	21.6	443.1	618.2	22.5	1.40	22.4

subcooler plus the internal heat exchanger of 13.4 % for climatic class 3 conditions, 16.6 % for climatic class 4 conditions and 22.4 % for climatic class 7 conditions. Regarding the coefficient of performance, the combination of thermoelectric subcooler plus internal heat exchanger enhances the coefficient of performance in comparison with the base cycle by 12.6 %, 16.9 % and 22.5 % for climatic class 3, 4 and 7 conditions, respectively. Lastly, the easy control of the thermoelectric subcooler adds flexibility to the refrigeration system, being able to increase the cooling capacity of the system for short periods of time to match the cooling demands of the facility.

The novel combination of thermoelectric subcooler plus internal heat exchanger presented in this work outperforms each of the technologies on their own and experimentally demonstrates that this combination of technologies is a great solution to improve the coefficient of performance of carbon dioxide refrigeration cycles. In addition, the combination increases the cooling capacity and capabilities of transcritical carbon dioxide refrigeration cycles. Moreover, the increase in coefficient of performance turns directly into a reduction of the energy consumption of the system and a decrease in the indirect effect of greenhouse gases emissions of the refrigeration facility. Lastly, the proposed combination of technologies is presented as a robust, compact, modular and promising novel solution suitable to boost the performance of low–medium power transcritical carbon dioxide refrigeration systems.

CRediT authorship contribution statement

Álvaro Casi: Methodology, Validation, Investigation, Writing – original draft. **Patricia Aranguren:** Validation, Formal analysis, Data curation. **Miguel Araiz:** Methodology, Writing – review & editing. **Daniel Sanchez:** Investigation, Data curation. **Ramon Cabello:** Supervision, Project administration. **David Astrain:** Resources, Writing – review & editing.

Declaration of competing interest

The authors declare that they have no known competing financial interests or personal relationships that could have appeared to influence the work reported in this paper.

Data availability

The authors are unable or have chosen not to specify which data has been used.

Acknowledgements

The authors would like to acknowledge the support of the Spanish Ministry of Science, Innovation and Universities, and European Regional Development Fund, for the funding under the RTI2018-093501-B-C21 and RTI2018-093501-B-C22 research projects. We would also like to acknowledge the support from the Education Department of the Government of Navarra with the *Predoctoral Grants for Phd programms of Interest to Navarra* and the Official School of Industrial Engineers of Navarre with the scholarship *Fuentes Dutor*. Publication funding provided by Universidad Pública de Navarra.

References

[1] Intergovernmental Panel on Climate Change. Climate change 2021 the physical science basis. 2021.
[2] United Nations. Emissions gap report 2021. 2021.
[3] International Institute of Refrigeration. 35th informatory note on refrigeration technologies / the impact of the refrigeration sector on climate change. 2017.
[4] International Institute of Refrigeration. 38th informatory note on refrigeration technologies / the role of refrigeration in the global economy. 2019.
[5] Parties to the Montreal Protocol. Kigali amendment to the montreal protocol on substances that deplete the ozone layer. 2016, 2016.
[6] European Parliament and the Council of the European Union. Regulation (EU) No 517/2014 of the European parliament and of the council of 16 April 2014 on fluorinated greenhouse gases and repealing regulation (EC) No 842/2006. Oficial J Eur Union 2014.
[7] Lorentzen G. The use of natural refrigerants: a complete solution to the CFC/HCFC predicament. Int J Refrig 1995;18.
[8] Kim MH, Pettersen J, Bullard CW. Fundamental process and system design issues in CO2 vapor compression systems. Prog Energy Combust Sci 2004;30:119–74. http://dx.doi.org/10.1016/j.pecs.2003.09.002.
[9] Zhu Y, Li C, Zhang F, Jiang PX. Comprehensive experimental study on a transcritical CO2 ejector-expansion refrigeration system. Energy Convers Manage 2017;151:98–106. http://dx.doi.org/10.1016/j.enconman.2017.08.061.
[10] Llopis R, Nebot-Andrés L, Cabello R, Sánchez D, Catalán-Gil J. Évaluation expérimentale d'une installation frigorifique transcritique au CO2 avec un sous-refroidissement mécanique dédié. Int J Refrig 2016;69:361–8. http://dx.doi.org/10.1016/j.ijrefrig.2016.06.009.
[11] Sánchez D, Catalán-Gil J, Cabello R, Calleja-Anta D, Llopis R, Nebot-Andrés L. Experimental analysis and optimization of an R744 transcritical cycle working with a mechanical subcooling system. Energies 2020;13. http://dx.doi.org/10.3390/en13123204.
[12] Sarkar J, Agrawal N. Performance optimization of transcritical CO2 cycle with parallel compression economization. Int J Therm Sci 2010;49:838–43. http://dx.doi.org/10.1016/j.ijthermalsci.2009.12.001.
[13] Chesi A, Esposito F, Ferrara G, Ferrari L. Experimental analysis of R744 parallel compression cycle. Appl Energy 2014;135:274–85. http://dx.doi.org/10.1016/j.apenergy.2014.08.087.
[14] Megdouli K, Sahli H, Tashtoush BM, Nahdi E, Kairouani L. Theoretical research of the performance of a novel enhanced transcritical CO2 refrigeration cycle for power and cold generation. Energy Convers Manage 2019;201. http://dx.doi.org/10.1016/j.enconman.2019.112139.
[15] Catalán-Gil J, Nebot-Andrés L, Sánchez D, Llopis R, Cabello R, Calleja-Anta D. Improvements in CO2 booster architectures with different economizer arrangements. Energies 2020;13. http://dx.doi.org/10.3390/en13051271.
[16] Sharma S, Dwivedi VK, Pandit SN. A review of thermoelectric devices for cooling applications. Int J Green Energy 2014;11:899–909. http://dx.doi.org/10.1080/15435075.2013.829778.
[17] Liu X, Fu R, Wang Z, Lin L, Sun Z, Li X. Thermodynamic analysis of transcritical CO2 refrigeration cycle integrated with thermoelectric subcooler and ejector. Energy Convers Manage 2019;188:354–65. http://dx.doi.org/10.1016/j.enconman.2019.02.088.

[18] Sánchez D, Aranguren P, Casi A, Llopis R, Cabello R, Astrain D. Experimental enhancement of a CO2 transcritical refrigerating plant including thermoelectric subcooling. Int J Refrig 2020;120:178–87. http://dx.doi.org/10.1016/j.ijrefrig.2020.08.031.

[19] Aranguren P, Sánchez D, Casi A, Cabello R, Astrain D. Experimental assessment of a thermoelectric subcooler included in a transcritical CO2 refrigeration plant. Appl Therm Eng 2021;190. http://dx.doi.org/10.1016/j.applthermaleng.2021.116826.

[20] Torrella E, Sánchez D, Llopis R, Cabello R. Energetic evaluation of an internal heat exchanger in a CO2 transcritical refrigeration plant using experimental data. Int J Refrig 2011;34:40–9. http://dx.doi.org/10.1016/j.ijrefrig.2010.07.006.

[21] Sánchez D, Patiño J, Llopis R, Cabello R, Torrella E, Fuentes FV. New positions for an internal heat exchanger in a CO2 supercritical refrigeration plant. Experimental analysis and energetic evaluation. Appl Therm Eng 2014;63:129–39. http://dx.doi.org/10.1016/j.applthermaleng.2013.10.061.

[22] Kwan TH, Shen Y, Wu Z, Yao Q. Performance analysis of the thermoelectric device as the internal heat exchanger of the trans-critical carbon dioxide cycle. Energy Convers Manage 2020;208. http://dx.doi.org/10.1016/j.enconman.2020.112585.

[23] Casi Á, Aranguren P, Araiz M, Sanchez D, Cabello R, Astrain D. Experimental evaluation of a transcritical CO2 refrigeration facility working with an internal heat exchanger and a thermoelectric subcooler: Performance assessment and comparative. Int J Refrig 2022. http://dx.doi.org/10.1016/j.ijrefrig.2022.05.024.